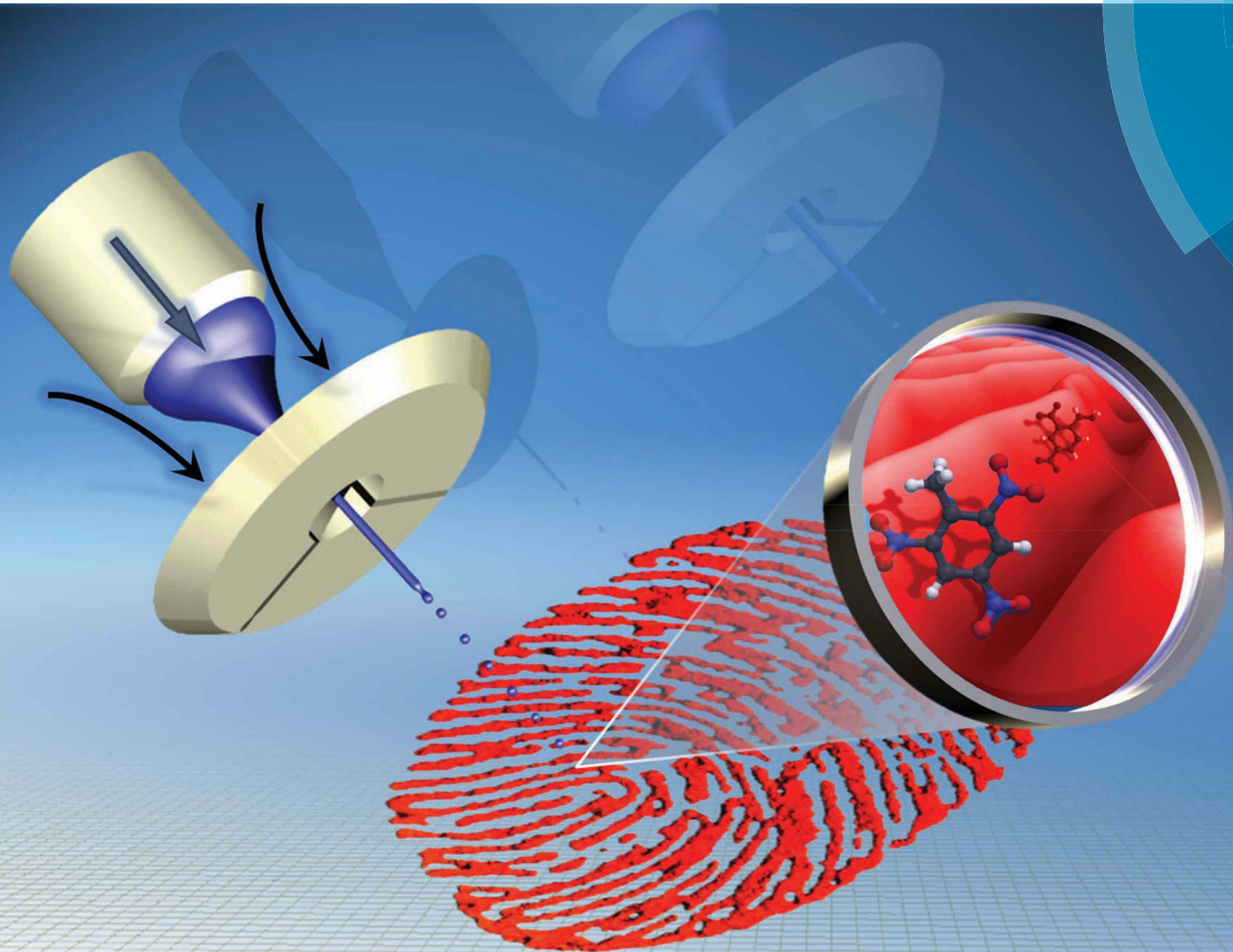


# Analyst

[www.rsc.org/analyst](http://www.rsc.org/analyst)



ISSN 0003-2654



## COMMUNICATION

Thomas P. Forbes and Edward Sisco  
Chemical imaging of artificial fingerprints by desorption electro-flow focusing ionization mass spectrometry

# Chemical imaging of artificial fingerprints by desorption electro-flow focusing ionization mass spectrometry†‡

Cite this: *Analyst*, 2014, 139, 2982Received 23rd January 2014  
Accepted 17th February 2014

DOI: 10.1039/c4an00172a

www.rsc.org/analyst

Thomas P. Forbes<sup>\*a</sup> and Edward Sisco<sup>b</sup>

Desorption electro-flow focusing ionization (DEFFI) mass spectrometry was used to image chemical distributions of endogenous, *e.g.*, fatty acids, and trace exogenous compounds, *e.g.*, explosives, narcotics and lotions, in deposited and lifted artificial fingerprints, directly from forensic lift tape. An artificial fingerprint mold and synthetic fingerprint material were incorporated for the controlled deposition of material for technique demonstration and evaluation.

The development of mass spectrometry imaging (MSI) has provided a powerful tool for the forensic analysis of spatial chemical distributions in latent fingerprints. Mass spectrometry offers a breadth of information, enabling the direct determination of the analyte's nominal mass as well as structural information through the analysis of molecular fragments. The chemical distributions of endogenous components, *i.e.*, eccrine and sebaceous secretions, and exogenous components, *i.e.*, explosives, narcotics, and other forensically relevant analytes, have been resolved in fingerprints using a range of techniques, including secondary ion mass spectrometry (SIMS),<sup>1–5</sup> matrix-assisted laser desorption ionization mass spectrometry (MALDI-MS),<sup>6</sup> and desorption electrospray ionization mass spectrometry (DESI-MS).<sup>7,8</sup> Here, we focus on ambient pressure ionization mass spectrometry imaging, for which recent reviews have been published.<sup>9</sup> Of the ambient pressure ionization techniques, chemical imaging with desorption electrospray ionization has experienced significant investigation,<sup>7,8,10–13</sup> most notably in the area of biological imaging.<sup>14,15</sup> For biological tissues, the high pressure pneumatic-assist gas generated by the

DESI source provides the necessary ablation of tissue for high sensitivity signal acquisition. However, for imaging fingerprints, the high pressure gas can result in unwanted redistribution or smearing of analytes on certain surfaces.<sup>8</sup>

Although latent fingerprints are deposited on a wide range of materials, they are often removed with forensic lift tape for further biometric analysis. In the present study, we demonstrated the proof-of-concept mass spectrometry imaging of chemical distributions within deposited and lifted artificial fingerprints, directly from lift tape, using desorption electro-flow focusing ionization (DEFFI). DEFFI-MSI, integrates the electro-flow focusing technique<sup>16,17</sup> in a desorption-style automated chemical imaging instrument. The development of DEFFI, including primary and secondary droplet charging and transmission characteristics,<sup>18</sup> mass spectrometric investigation of narcotics and explosives, and initial comparison to DESI can be found in the literature.<sup>19</sup> Briefly, DEFFI employs a recessed solvent capillary, around which a low pressure, *e.g.*, approximately 70 kPa to 140 kPa, laminar gas stream focuses the solvent stream through a small orifice (Fig. 1). The geometric configuration also enables interrogation in regimes including charged-droplet-based electrospray and corona discharge chemical ionization at potentials less than 1 kV.<sup>16,18,19</sup> This technique also benefits from rapid imaging under atmospheric conditions of samples with minimal or no sample preparation.

<sup>a</sup>National Institute of Standards and Technology, Materials Measurement Science Division, Gaithersburg, MD, USA. E-mail: thomas.forbes@nist.gov; Tel: +1-(301) 975-2111

<sup>b</sup>Department of Chemistry and Biochemistry, University of Maryland, College Park, MD, USA

† Electronic supplementary information (ESI) available: Additional experimental details, figures, mass spectra, and chemical images. See DOI: 10.1039/c4an00172a

‡ Official contribution of the National Institute of Standards and Technology; not subject to copyright in the United States.

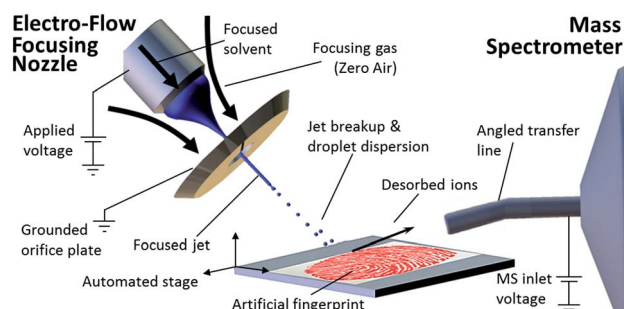


Fig. 1 Schematic representation of the desorption electro-flow focusing ionization (DEFFI) mass spectrometry imaging setup.

The chemical distributions investigated in this study were generated by an artificial fingerprint mold (Fig. S1, ESI†) and synthetic fingerprint material comprised of endogenous components, including common eccrine and sebaceous secretions (Fig. S3, ESI†).<sup>20,21</sup> The artificial fingerprint mold and material provided a precisely controlled system for device and technique development, characterization, and optimization. The amounts and deposition of synthetic endogenous material were specifically controlled, eliminating sample-to-sample variability as experienced with genuine fingerprints. Investigations into the natural distribution of analytes in latent fingerprints and the direct analysis from forensic lift tapes may improve the validation of trace detection technologies and provide “signatures”, indicating the method and conditions of deposition.

The MSI system comprised of the DEFFI source coupled to an automated 2-axis stage and a 4000 QTrap® Triple-Quadrupole MS system§ (Applied Biosystems/MDS Sciex, Foster City, CA/Toronto, Canada) with an extended 36 mm, 15° angle capillary interface (Fig. 1 and S2, ESI†). The DEFFI ion source, consisting of an electro-Flow Focusing® nebulizer (Ingeniatics Tecnológicas, Sevilla, Spain), was oriented less than 1 mm above the sample substrate at an incidence angle of 50° with respect to the sample. Details of the DEFFI source parameters and operation were described elsewhere (ESI†).<sup>19</sup> The artificial fingerprint, synthetic fingerprint material, and analyte of interest were deposited onto, or lifted from a primary substrate surface, with forensic lift tape (Sirchie® Fingerprint Laboratories, Youngsville, NC). The actual artificial fingerprint mold was approximately 16 mm × 21 mm, comparable in size to average fingerprints.<sup>22</sup> In each case, a relevant amount of target analyte, *i.e.*, 5 µg,<sup>7,23</sup> and 5 µg of synthetic fingerprint material were deposited onto the artificial fingerprint mold (on the order of 10 ng mm<sup>-2</sup>), however this represented an upper limit, as the aliquot of material deposited in each stamp or lifted from a deposited print was not directly determined. The acquired mass spectra and chemical distribution data were imaged with the MATLAB-based freeware package, MSiReader (v0.04, W. M. Keck FT-ICR Mass Spectrometry Laboratory, North Carolina State University).<sup>24</sup>

Fig. 2 displays the chemical distributions of oleic acid, a fatty acid component of the synthetic endogenous fingerprint material, and octahydro-1,3,5,7-tetranitro-1,3,5,7-tetrazocine (HMX), a nitroamine explosive, for a fingerprint deposited directly onto forensic lift tape and interrogated in negative mode. Oleic acid was imaged as a gauge of the actual print distribution and location. Peaks for the deprotonated ion,  $m/z$  281 [M - H]<sup>-</sup>, the nitrite adduct,  $m/z$  328 [M + NO<sub>2</sub>]<sup>-</sup>, and the nitrate adduct,  $m/z$  344 [M + NO<sub>3</sub>]<sup>-</sup> were observed (Fig. 3(a) and S3, ESI†). The DEFFI source has demonstrated a propensity to generate nitrate ions in negative mode, commonly resulting in nitrate adducts.<sup>19</sup> In addition, when choosing indicator components of the simulated fingerprint, the background generated by the forensic lift tape was taken into consideration (Fig. 3(c)–(d)). The Sirchie® lift tape displayed significant peaks from adhesive components at  $m/z$  (297, 311, 325 and 339) and  $m/z$  (245, 261, 462, 467 and 483) in negative and positive mode MS, respectively. The HMX explosive also demonstrated a strong nitrate adduct peak,  $m/z$  358 [M + NO<sub>3</sub>]<sup>-</sup>, and clear residue distribution (Fig. 2(b) and 3(b)).

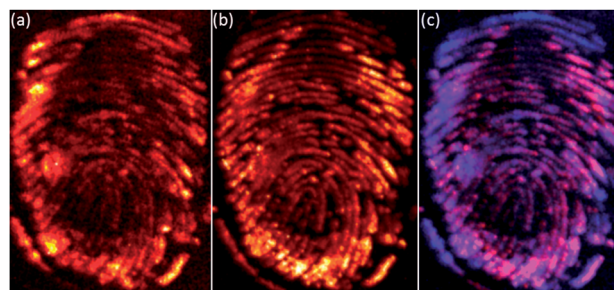


Fig. 2 Desorption electro-flow focusing ionization mass spectrometry images of an HMX-laden artificial fingerprint deposited onto forensic lift tape. Chemical images of (a) oleic acid, a component of the synthetic endogenous material ( $m/z$  344 [M + NO<sub>3</sub>]<sup>-</sup>), and (b) HMX ( $m/z$  358 [M + NO<sub>3</sub>]<sup>-</sup>). Lighter color indicates higher intensity. (c) A colocalization map of the fingerprint indicator, oleic acid (blue) and HMX explosive (red).

DEFFI was able to provide clear images of trace exogenous components without being obscured by the tape or artificial fingerprint material. The colocalization map in Fig. 2(c) displays the relative distributions of the synthetic fingerprint material, represented by the oleic acid distribution, and HMX explosive. The low pressure operation of DEFFI, relative to DESI, minimized redistribution of analyte and Fig. 2 clearly demonstrates the ability to image endogenous and exogenous materials and resolve ridge detail of artificially created fingerprints.

The experiment conducted above was repeated in positive mode considering a fingerprint comprised of the synthetic fingerprint material, including an additional common hand lotion (Gold Bond Ultimate Hand Sanitizer Sheer Moisture), and methamphetamine. Fig. 4 displays the chemical distributions of benzethonium, an easily ionized component of the hand lotion, and the narcotic methamphetamine. Benzethonium chloride, a quaternary ammonium salt, was the active anti-microbial ingredient in the Gold Bond lotion. The molecular cation of benzethonium,  $m/z$  412 [M]<sup>+</sup>, provided a strong and readily tractable peak from the Gold Bond lotion (Fig. S4, ESI†) and clear image of the fingerprint location and distribution. The methamphetamine distribution was dominated by the protonated molecule,  $m/z$  150 [M + H]<sup>+</sup> (Fig. S4, ESI†). As displayed in Fig. 4(b), methamphetamine experienced significant signal suppression in positive mode. Ion suppression effects are common in mass spectrometry and have been demonstrated for similar techniques such as electrospray ionization (ESI), DESI, and SIMS.<sup>7</sup> Determination of the appropriate source solvent, mass spectrometry mode, and geometrical configuration are all necessary for optimal detection and imaging of the specific analyte of interest. Fig. 4(c) demonstrates a colocalization map of the artificial fingerprint and methamphetamine distribution. DEFFI's combination of charge droplet electrospraying and corona discharge-based chemical ionization enabled efficient ionization and imaging in both negative and positive mode MS.

Finally, artificial fingerprints were deposited onto a representative automobile surface, comprised of an aluminum substrate that was painted black and then clear-coated. The latent prints were then lifted with forensic lift tape and directly

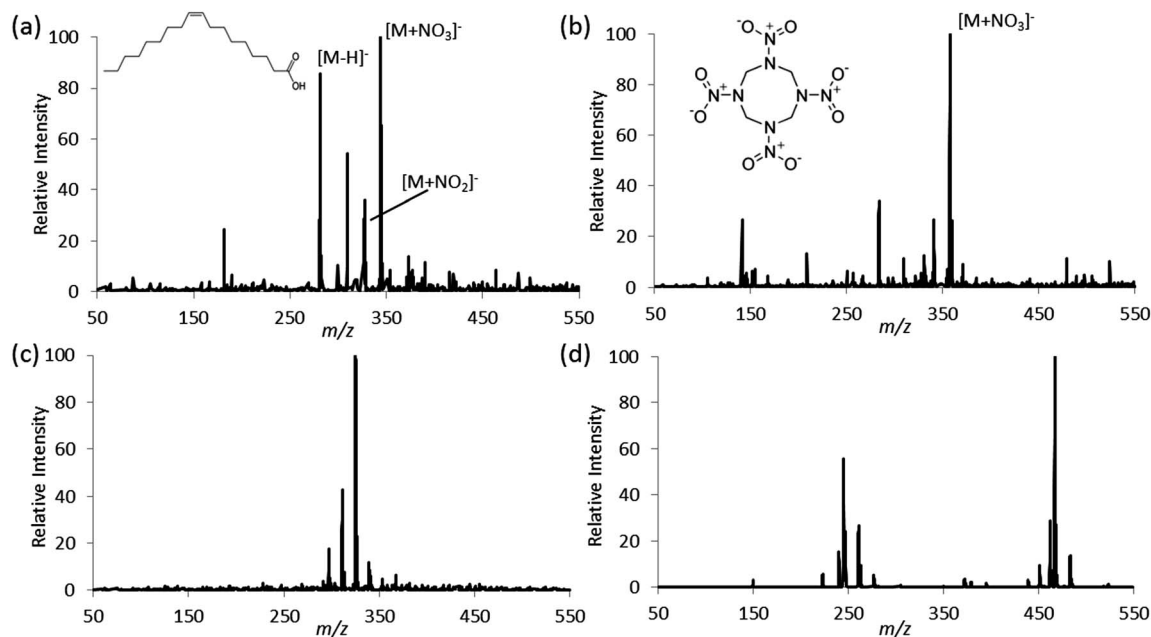


Fig. 3 Background-subtracted, individual component, DEFFI mass spectra for (a) oleic acid and (b) HMX, in negative mode MS. Each analyte was sampled and spectra were summed for 30 s. Insets: chemical structure of oleic acid and HMX. Representative DEFFI background mass spectra for the Sirchie® fingerprint lift tape in (c) negative and (d) positive mode MS.

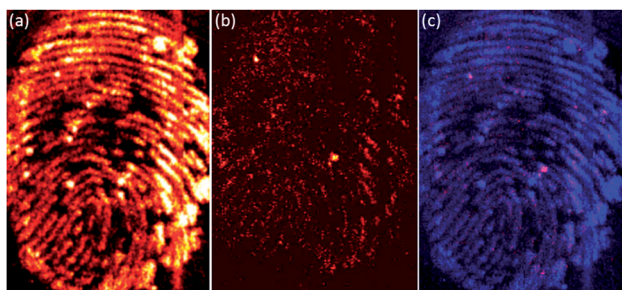


Fig. 4 Desorption electro-flow focusing ionization mass spectrometry images of a methamphetamine-laden artificial fingerprint deposited onto forensic lift tape. Chemical images of (a) benzethonium, a component of lotion spiked into the synthetic fingerprint material ( $m/z$  412  $[M]^+$ ), and (b) methamphetamine ( $m/z$  150  $[M+H]^+$ ). Lighter color indicates higher intensity. (c) A colocalization map of the fingerprint material indicator, benzethonium (blue) and the narcotic methamphetamine (red).

analyzed without further preparation. The chemical distributions of artificial fingerprint material components and trace exogenous compounds of lifted prints were imaged in negative and positive mode (Fig. 5 and S6†). Fig. 5 displays chemical images for a lifted artificial fingerprint laden with the explosive 1,3,5-trinitroperhydro-1,3,5-triazine (RDX). The distributions of palmitoleic acid, another fatty acid component of the synthetic fingerprint material, and the RDX nitrate adduct were imaged. DEFFI ionization of palmitoleic acid also exhibited peaks for the deprotonated ion,  $m/z$  253  $[M-H]^-$ , the nitrate adduct,  $m/z$  316  $[M+NO_3]^-$ , and the dimer,  $m/z$  507  $[2M-H]^-$  (Fig. S5 and S6, ESI†). Fig. 5(a) displays the chemical image of the deprotonated ion of palmitoleic acid. Strong signals for the RDX monomer

and dimer adducts with nitrate were observed (Fig. S5 and S6, ESI†), as expected and previously demonstrated in the literature.<sup>19</sup> The colocalization map in Fig. 5(c) shows the resolved ridge detail of the synthetic fingerprint material, *i.e.*, palmitoleic acid, and the RDX monomer and dimer nitrate adducts (Fig. S6, ESI†). The capacity to image multiple chemical components of a latent fingerprint may provide a direct means to image poorly developed fingerprints. Here, the fatty acid component provided a lower resolution image than the RDX component; the combination of the two may enhance the image resolution of any individual component.

Positive mode chemical images for a lifted artificial fingerprint spiked with Gold Bond lotion, as seen above, and the narcotic, cocaine, were also acquired (Fig. S7, ESI†). Again,

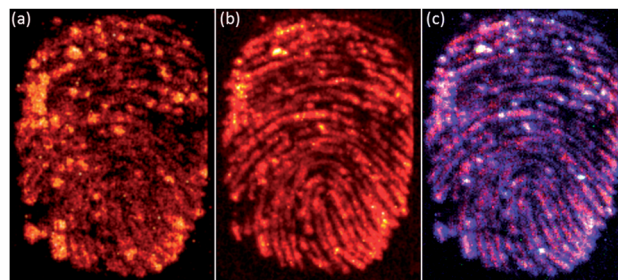


Fig. 5 Desorption electro-flow focusing ionization mass spectrometry images of an RDX-laden artificial fingerprint deposited onto black-painted, clear-coat finished, aluminum substrate and pulled with forensic lift tape. Chemical images of (a) palmitoleic acid, a component of the synthetic endogenous material ( $m/z$  253  $[M-H]^-$ ) and (b) RDX monomer nitrate adduct ( $m/z$  284  $[M+NO_3]^-$ ). (c) A colocalization map of the fingerprint material indicator, palmitoleic acid (blue), and the RDX explosive (red).

components of the lotion, *i.e.*, the molecular ions of benzenonium ( $m/z$  412  $[M]^+$ ) and behentrimonium ( $m/z$  368  $[M]^+$ ), provided strong print indicators (Fig. S4 and S7, ESI<sup>†</sup>). The cocaine distribution was dominated by the protonated molecules,  $m/z$  304  $[M + H]^+$ . The colocalization map shows the resolved ridge detail of the artificial fingerprint material, *i.e.*, lotion, and cocaine (Fig. S7, ESI<sup>†</sup>). Comparing the chemical images in Fig. 2 through 5, the lift process created notable reduction in the ridge detail and overall fingerprint resolution. The ability to smoothly lift the print without smearing played a significant role in the final resolution of the lifted print and image. In addition, significant levels of fingerprint material remained on the aluminum substrate following the print lift process (Fig. S8, ESI<sup>†</sup>). A cyanoacrylate fuming enhancement of the lifted artificial fingerprints demonstrated that a nontrivial amount of material and ridge detail still remained for post processing, following DEFFI imaging (Fig. S9, ESI<sup>†</sup>).

The results presented show the use of desorption electroflow focusing ionization (DEFFI) mass spectrometry imaging for the visualization of chemical distributions within artificial fingerprints. As compared to DESI, DEFFI provided a unique combination of low applied pressure and applied potential operation, electrospray and chemical ionization, and minimal sample redistribution, in both positive and negative mode MS. The direct production of nitrate ions within the DEFFI source, also supported stable adduct formation with both fatty acids and explosive molecules. Chemical distributions from artificial fingerprints lifted directly from clear-coated aluminum were imaged. The DEFFI-MSI process also enabled the post-process cyanoacrylate development of imaged prints. Future work will also consider utilizing MS/MS or multiple reaction monitoring transition imaging to mitigate any background effects in resolution, as well as investigating methods to quantify the exogenous material. The artificial fingerprints, developed with a mold and synthetic fingerprint material of common eccrine and sebaceous secretions, enable further investigation of a controlled system for more universal comparison and evaluation of techniques. The mass spectrometry imaging (MSI) system described here will be used for future characterization of trace residues and particle distributions within fingerprints by multiple ionization sources, *e.g.*, DEFFI, DESI, and LTP. Immediate control over the fingerprint ridge detail, amount of endogenous and exogenous material, and deposition or lift method will enable direct comparisons for these sources.

## Acknowledgements

The authors thank Matthew Staymates, Dr Shin Muramoto, and Dr Greg Gillen at the National Institute of Standards and Technology for their technical help with the LabVIEW code and stimulating discussions, respectively. ES acknowledges support from a Department of Defense Science, Mathematics, and Research for Transformation Fellowship. The U.S. Department of Homeland Security Science and Technology Directorate sponsored a portion of the production of this material under Interagency Agreement IAA HSHQDC-12-X-00024 with the National Institute of Standards and Technology.

## Notes and references

§ Certain commercial products are identified in order to adequately specify the procedure; this does not imply endorsement or recommendation by NIST, nor does it imply that such products are necessarily the best available for the purpose.

- 1 M. J. Bailey, M. Ismail, S. Bleay, N. Bright, M. L. Elad, Y. Cohen, B. Geller, D. Everson, C. Costa, R. P. Webb, J. F. Watts and M. de Puit, *Analyst*, 2013, **138**, 6246–6250.
- 2 N. J. Bright, R. P. Webb, S. Bleay, S. Hinder, N. I. Ward, J. F. Watts, K. J. Kirkby and M. J. Bailey, *Anal. Chem.*, 2012, **84**, 4083–4087.
- 3 E. Sisco, L. T. Demoranville and G. Gillen, *Forensic Sci. Int.*, 2013, **231**, 263–269.
- 4 M. I. Szyrkowska, K. Czernski, J. Grams, T. Paryjczak and A. Parczewski, *Imaging Sci. J.*, 2007, **55**, 180–187.
- 5 M. I. Szyrkowska, K. Czernski, J. Rogowski, T. Paryjczak and A. Parczewski, *Forensic Sci. Int.*, 2009, **184**, e24–e26.
- 6 R. Wolstenholme, R. Bradshaw, M. R. Clench and S. Francese, *Rapid Commun. Mass Spectrom.*, 2009, **23**, 3031–3039.
- 7 D. R. Ifa, N. E. Manicke, A. L. Dill and R. G. Cooks, *Science*, 2008, **321**, 805.
- 8 M. F. Mirabelli, A. Chramow, E. C. Cabral and D. R. Ifa, *J. Mass Spectrom.*, 2013, **48**, 774–778.
- 9 C. Wu, A. L. Dill, L. S. Eberlin, R. G. Cooks and D. R. Ifa, *Mass Spectrom. Rev.*, 2013, **32**, 218–243.
- 10 D. R. Ifa, L. M. Gumaelius, L. S. Eberlin, N. E. Manicke and R. G. Cooks, *Analyst*, 2007, **132**, 461–467.
- 11 D. R. Ifa, J. M. Wiseman, Q. Song and R. G. Cooks, *Int. J. Mass Spectrom.*, 2007, **259**, 8–15.
- 12 V. Kertesz and G. J. Van Berkel, *Rapid Commun. Mass Spectrom.*, 2008, **22**, 2639–2644.
- 13 V. Kertesz and G. J. Van Berkel, *Anal. Chem.*, 2008, **80**, 1027–1032.
- 14 D. Campbell, C. Ferreira, L. Eberlin and R. G. Cooks, *Anal. Bioanal. Chem.*, 2012, **404**, 389–398.
- 15 J. M. Wiseman, D. R. Ifa, Q. Song and R. G. Cooks, *Angew. Chem., Int. Ed.*, 2006, **45**, 7188–7192.
- 16 A. M. Gañán-Calvo, J. M. Lopez-Herrera and P. Riesco-Chueca, *J. Fluid Mech.*, 2006, **566**, 421–445.
- 17 A. M. Gañán-Calvo and J. M. Montanero, *Phys. Rev. E: Stat., Nonlinear, Soft Matter Phys.*, 2009, **79**, 066305.
- 18 T. P. Forbes, T. M. Brewer and G. Gillen, *Appl. Phys. Lett.*, 2013, **102**, 214102.
- 19 T. P. Forbes, T. M. Brewer and G. Gillen, *Analyst*, 2013, **138**, 5665–5673.
- 20 E. Sisco, J. L. Staymates, K. Schilling and G. Gillen, 2014, unpublished.
- 21 J. L. Staymates, M. E. Staymates and G. Gillen, *Anal. Methods*, 2013, **5**, 180–186.
- 22 J. C. Wu, in *Statistical Analysis of Widths and Heights of Images from Segmentation Data*, 2008, vol. 2008, <http://biometrics.nist.gov/>.
- 23 J. Bohannon, *Science*, 2007, **316**, 42–44.
- 24 G. Robichaud, K. Garrard, J. Barry and D. Muddiman, *J. Am. Soc. Mass Spectrom.*, 2013, **24**, 718–721.